DOI: 10.1002/asia.200600429

Self-Assembly and Host–Guest Chemistry of a 3.5-nm Coordination Nanotube

Takumi Yamaguchi,[a] Shohei Tashiro,[a] Masahide Tominaga,[a] Masaki Kawano,[a] Tomoji Ozeki,[b] and Makoto Fujita*[a]

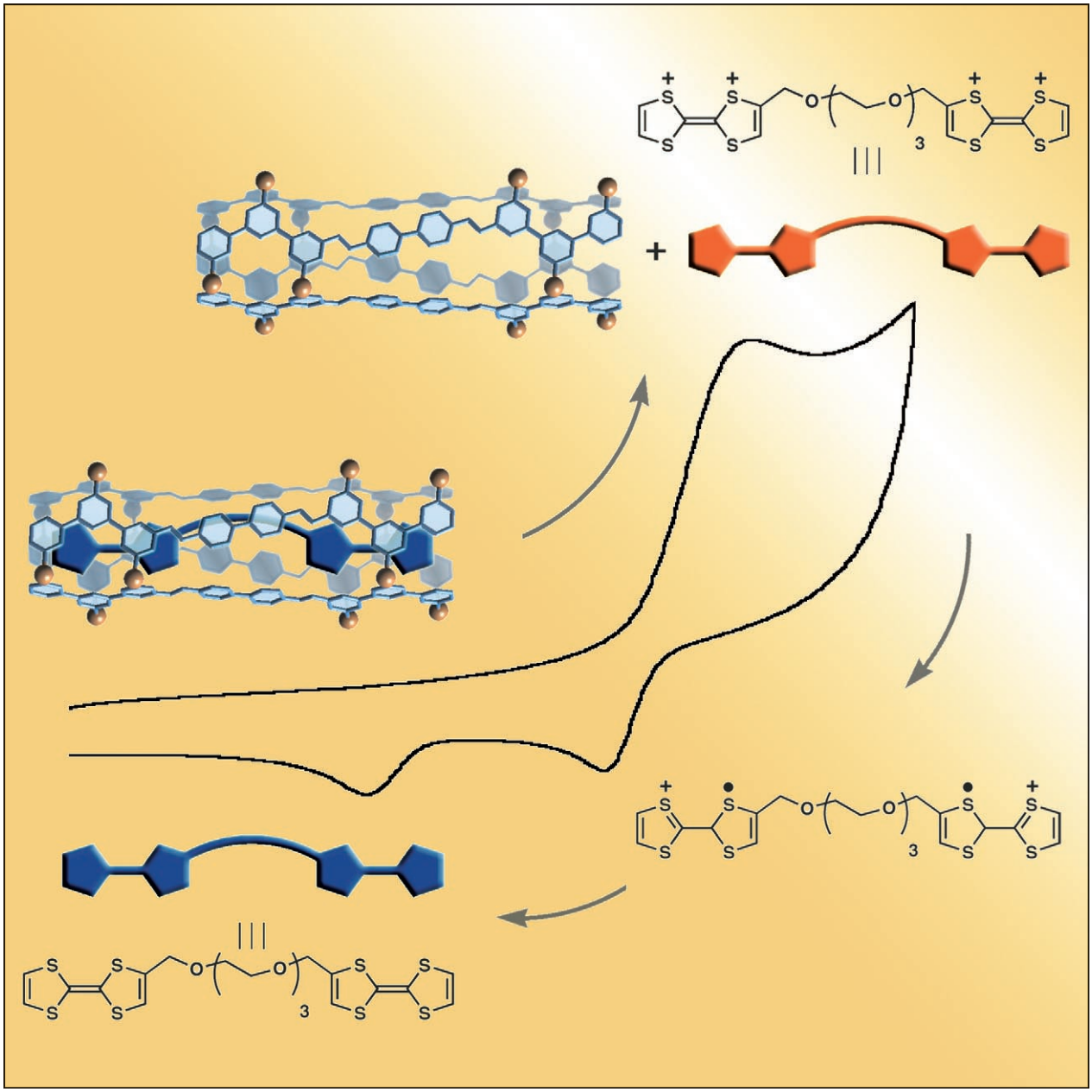

Abstract: Upon complexation with Pd^{II} ions, precisely designed strandlike ligands with two tris(3,5-pyridine) units at both terminals were assembled, with the aid of a linear template molecule, into a discrete tubular complex with a length of 3.5 nm. The high stability and the well-defined structure of the coordination nanotube were revealed by NMR spectroscopy, cold-spray ionization MS, and single-crystal X-ray analysis. Guest lengths were discriminated by the tube: When the association of strandlike guest molecules, in which two biphenylene units are linked with an $(OCH_2CH_2)_n$ linker, were compared, the tube selectively recognized an appropriate guest whose length was comparable to that of the tube. Tetrathiafulvalene (TTF)-terminated linear guests were directly oxidized to TTF^{2+} in the tube, but reduced stepwise via $TTF^{+\cdot}$ outside the tube.

Keywords: host–guest systems · nanotubes · palladium · self-assembly · template synthesis

Introduction

The tube structure is one of the most basic and unique frameworks that attract considerable current interest in broad scientific areas because of their potential abilities for selective inclusion or transportation of ions and molecules and for specific chemical transformations. In biology, extensive studies have been made on tubular proteins that exist in biological membranes as ion channels.[1] In physics and materials science, carbon nanotubes[2] are of special interest in the development of new basic materials. Therefore, to explore the potential functions and applications of tubes, the chemical construction of tubes based on precise design at the molecular level is particularly important.

Recently, molecular self-assembly has provided rather efficient approaches to well-defined tubular structures.[3–9] Linking tapelike molecules into cylindrical shapes is one of the most efficient approaches that make possible the strict control of tube length and diameter (Scheme 1). According to this strategy, we designed tapelike ligand **1** and synthesized 3.5-nm-sized coordination nanotube **2** from four ligands and twelve $[(en)Pd(NO_3)_2]$ coordination blocks.[10] The length of this ligand in its extended form is directly transferred to that of the tube that assembles with the aid of the remarkable template effect of 3.0-nm guest molecule **3**. Besides its facile preparation and definite structure, the high stability of **2** caused by 24 Pd^{II}–pyridine interactions permits

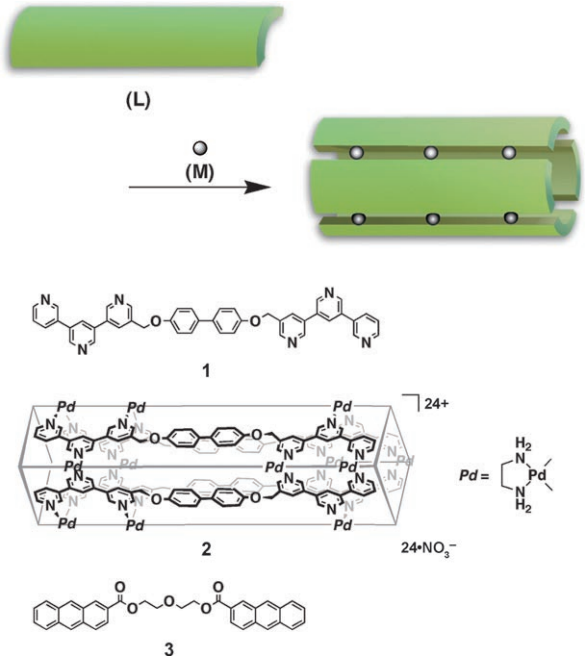

Scheme 1. Self-assembly of a coordination nanotube.

[a] T. Yamaguchi, Dr. S. Tashiro,[+] Dr. M. Tominaga,[++] Dr. M. Kawano, Prof. Dr. M. Fujita
Department of Applied Chemistry
School of Engineering, The University of Tokyo
and
CREST, Japan Science and Technology Agency
7-3-1 Hongo, Bunkyo-ku, Tokyo 113-8656 (Japan)
Fax: (+81) 3-5841-7257
E-mail: mfujita@appchem.t.u-tokyo.ac.jp

[b] Dr. T. Ozeki
Department of Chemistry and Materials Science
Tokyo Institute of Technology
2-12-1 O-okayama, Meguro-ku, Tokyo 152-8551 (Japan)

[+] Present address:
Department of Chemistry
School of Science, The University of Tokyo
7-3-1 Hongo, Bunkyo-ku, Tokyo 113-8656 (Japan)

[++] Present address:
Department of Pharmaceutical Technology
Faculty of Pharmaceutical Science at Kagawa Campus
Tokushima Bunri University
1314-1 Shido, Sanuki, Kagawa 769-2193 (Japan)

Supporting information for this article is available on the WWW under http://www.chemasianj.org or from the author.

the development of specific functions of the tube by exploiting its interior space. In this paper, we report the inclusion of linear-strand molecules by the tube and length discrimination in the inclusion process. We also discuss the binding and the unique redox behavior of linear guests with two tetrathiafulvalene (TTF) units at its ends.

Results and Discussion

Design and Synthesis of Ligand 1

We previously reported that pentakis(3,5-pyridine) ligands assemble into 2-nm-sized $M_{10}L_4$ coordination tubes.[9] The elongation of the tube by simply increasing the number of pyridine rings of the ligand was, however, unsuccessful because of very poor solubility of such ligands. Therefore, we developed a flexible molecular tape in which two tris(3,5-pyridine) units are connected by a linker. The selection of the linker is the key to the efficient formation of a long coordination tube. The ligand with a flexible alkyl linker ($-(CH_2)_4-$) adopted a U-shaped conformation. Even when a phenylene spacer was incorporated, the ligand dimerized into an M_6L_2 short tubular structure upon complexation with [(en)Pd(NO_3)$_2$] because of the U-shaped orientation.[11] To avoid this U-shaped intramolecular coordination, we designed ligand **1**, which has a rigid biphenylene spacer.

Ligand **1** was synthesized in two steps from 4,4′-dihydroxybiphenyl (Scheme 2), that is, the alkylation of 4,4′-dihydroxybiphenyl with 3-bromo-5-chloromethylpyridine (K_2CO_3, dry *N*,*N*-dimethylformamide (DMF), 5 days at 70 °C; 62 % yield) followed by Stille coupling with 3-tributylstannyl-5,3′-bipyridine ([Pd(PPh_3)$_4$], dry toluene, 5 days under reflux; 38 % yield).

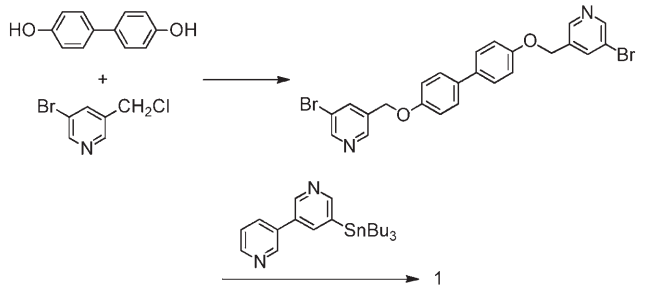

Scheme 2. Synthesis of ligand **1**.

Abstract in Japanese:

配位子の合理設計により、3.5-nm 長の配位結合ナノチューブの自己集合を達成した。２つのトリス（3,5-ピリジン）単位をビフェニレン基で連結した短冊状配位子を、ゲスト分子の存在下、パラジウムイオンを用いて筒状に自己集合させることによりチューブ状錯体を定量的に合成した。この構造を各種 NMR、CSI-MS および単結晶 X 線結晶構造解析により明らかにした。このチューブ錯体は高いゲスト包接能を有しており、長さの異なる紐状分子を識別し、内部空孔へサイズ選択的に取り込むことが可能である。さらに熱や電気化学的刺激による、包接錯体の動的挙動を観測した。

Self-Assembly of Coordination Nanotube 2·3

The complexation of **1** with [(en)Pd(NO_3)$_2$] in D_2O/CD_3CN (1:1) resulted in a complex mixture (Figure 1a). However, we observed a remarkable template effect[12,13] of strand guest molecule **3** in the quantitative self-assembly of **1** into coordination tube **2·3**. In **3**, two anthracenecarbonyl moieties are linked by a diethylene glycol unit, which makes the guest the ideal length for fitting within tube **2**. Upon addition of powdered **3**, the conversion of the mixture into a single product was accomplished after 6 h at 70 °C. The NMR spectrum was consistent with the formation of tube **2** (Figure 1b). Twelve proton signals (Ha–Hl) that stem from half of the framework of **2** were clearly observed, whereas the methylene protons are diastereotopic in the tube structure and were thus observed as an AB quartet. Template **3** was observed symmetrically with a marked upfield shift (e.g., the aromatic protons of the anthracenecarbonyl portion were found at $\delta = 7.39$–4.98 ppm) that indicates the accommodation of **3** within the tube. Besides the satisfactory NMR spectroscopic data obtained, the formula of **2·3** was confirmed by cold-spray ionization mass spectrometry (CSI-MS) with a series of prominent peaks of $[M-(NO_3^-)_m]^{m+}$ ($m = 4$–9) (Figure 2). For example, the peak at $m/z = 1279.4$ is consistent with the formula of guest-incorporated $M_{12}L_4$ complex $[\mathbf{2{\cdot}3}-(NO_3^-)_5]^{5+}$.

Single-Crystal X-ray Analysis of 3.5-nm-Sized Tube 2·3

The structure of complex **2·3** was unambiguously determined by single-crystal X-ray diffraction. Single crystals were obtained by the slow evaporation of a solution of **2·3** over one month. With a CCD diffractometer and a conventional X-ray generator, we failed to collect sufficient diffraction data for structural analysis even at 80 K, because the crystal was weakly diffracted due to the presence of severely disordered solvent molecules and a large cell volume; in particular, the long *b* axis (122 Å) led to poor resolution of spots. However, synchrotron X-ray irradiation (high flux and low divergence) significantly improved the quality of the data, which were sufficient for structural analysis. The crystallographic analysis revealed the tubular structure of **2·3** with a length of 3.5 nm (Figure 3a). Each ligand adopts the most extended conformation, and the tube framework is slightly helical. Although two structural isomers A and B may exist depending on the orientation of the ligand (Figure 4), the crystallographic analysis displayed only isomer A, which was formed exclusively as revealed by NMR spectroscopy. This observation agrees with force-field calculations that predict isomer A to be more stable than B by 8 kcal mol^{-1}.[14]

Within the cavity of **2**, two anthracenecarbonyl moieties of **3** are gripped by four tris(3,5-pyridine) units that are held together by six Pd^{II} ions through π–π stacking and CH–π contact. The diethylene glycol linker is essential because the tube did not assemble efficiently when anthracene or anthracenecarboxylate was employed as a template. Pd^{II}-

CHEMISTRY
AN ASIAN JOURNAL

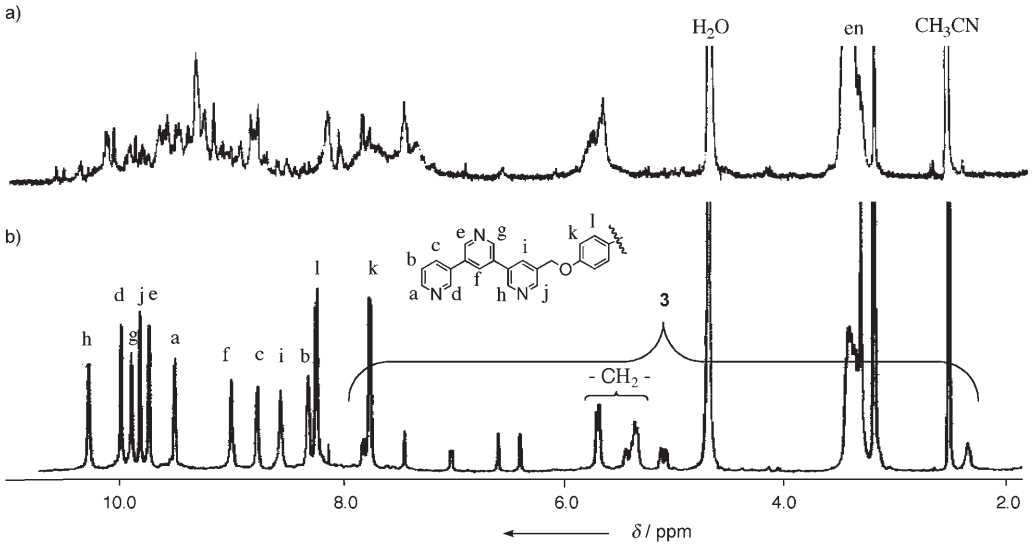

Figure 1. ^{1}H NMR spectroscopic observation of the guest-templated assembly of **2·3** (500 MHz, $D_2O/CD_3CN = 1:1$, 27 °C, tetramethylsilane (TMS)). a) Oligomeric mixture obtained from **1** and $[(en)Pd(NO_3)_2]$. b) Tubular structure **2·3** formed after addition of **3**.

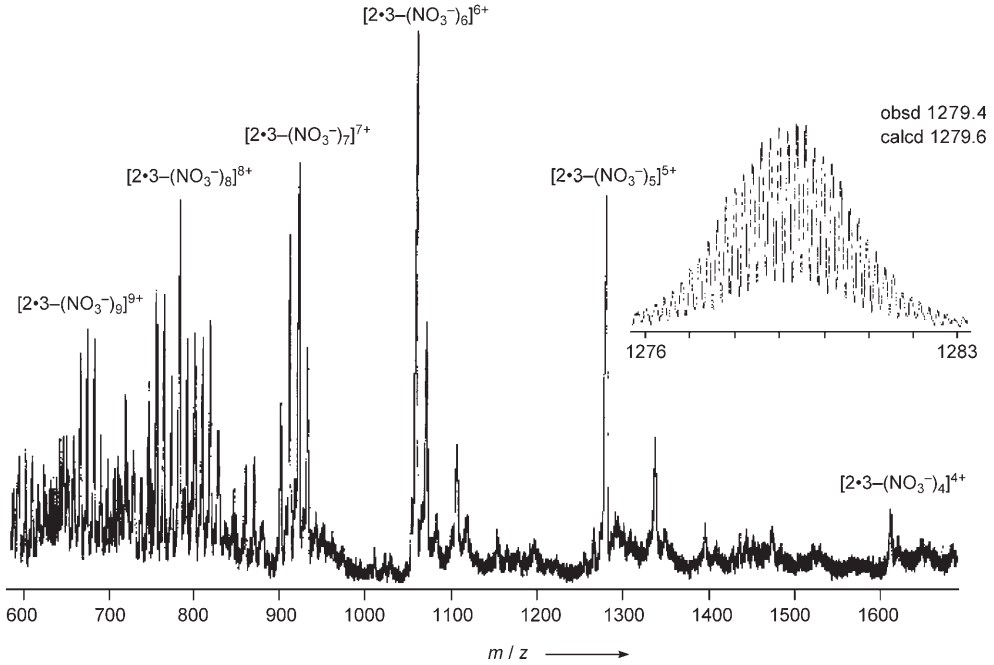

Figure 2. CSI-MS spectrum of **2·3** ($H_2O/CH_3CN/DMF = 1:1:0.03$). The prominent peaks of $[\mathbf{2·3}–(NO_3^-)_m+(DMF)_n]^{m+}$ ($m = 4$–9, $n = 0$–5) are clearly observed. The inset shows the isotopic pattern of the peak of $[\mathbf{2·3}–(NO_3^-)_5]^{5+}$.

linked tubular frameworks at both ends of **2** were probably simultaneously assembled through templating by the two anthracenecarbonyl moieties of **3**. Along the linear and slightly helical cavity of **2**, guest **3** adopts the most extended conformation with a twist of about 90°.

One-dimensional alignment of the tubes in the crystal packing is another intriguing feature revealed by the crystallographic analysis. In the crystal, all the tubes line up along the *b* axis of the unit cell to make infinite tubes (Figure 3b).[15] Channels that cross the infinite tube can be viewed in the *ac* plane (Figure 3c and d). The pyridine rings of the tube are stacked on the biphenylene group of an adjacent tube within the range of π–π interactions (3.4–3.7 Å).

Length Discrimination by Guest Binding

One of the most remarkable functions of the coordination nanotube is the strong binding of linear guest molecules in the tube. Guest binding by tube **2** is carried out by templating or guest exchange. Namely, a strand guest employed as a template can be exchanged by other linear guest molecules simply by suspending them in an aqueous solution of the

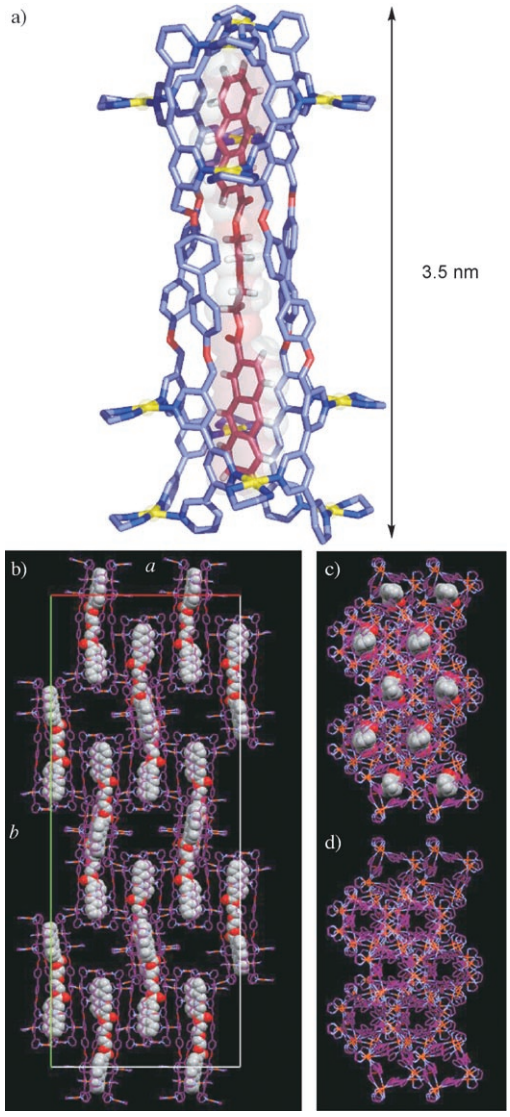

Figure 3. a) Crystal structure of **2·3**. b) The unit cell. c) and d) View of the tube along the crystallographic *b* axis. For clarity, H atoms, solvent molecules, anions, and guest molecules (in d)) are omitted.

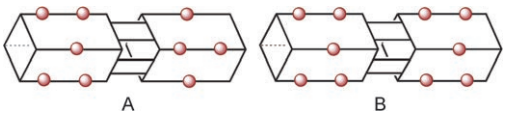

Figure 4. Schematic representation of the isomers of **2**.

tubular complex. In this guest exchange, we observed the discrimination of the guest length by the tube.[16] A linear guest of which length is comparable to that of the tube was found to be the most suitably bound in the tube.

We prepared strand molecules **4**, **5**, and **6**, in which two *p*-C_6H_5–C_6H_4 units are held together by an $(OCH_2CH_2)_n$ linker ($n=3$, 4, and 5, for **4**, **5**, and **6**, respectively). As revealed by NMR spectroscopic measurements, all the molecules efficiently templated the assembly of tube **2**: the reaction of ligand **1** with [(en)Pd(NO_3)$_2$] in the presence of **4**, **5**,

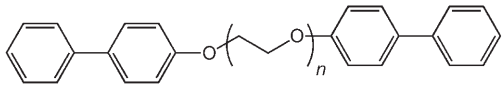

4: $n=3$
5: $n=4$
6: $n=5$

or **6** resulted in the formation of tube **2·4**, **2·5**, or **2·6**, respectively, in high yield (Figure 5a–c).

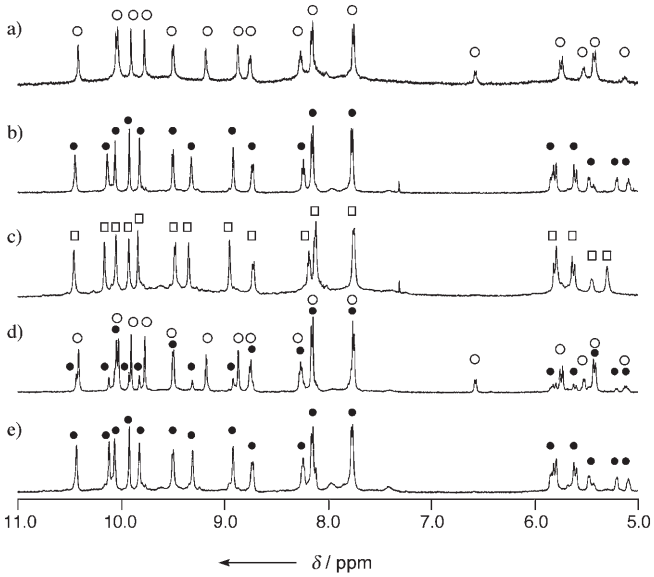

Figure 5. ^{1}H NMR spectroscopic observation of the size-selective recognition of strand molecules by the tube (500 MHz, $D_2O/CD_3CN=1:1$, 27 °C, TMS) showing the effective guest-templated assembly of a) **2·4**, b) **2·5**, and c) **2·6**. d) The mixture of ligand **1** (5.9 μmol) and [(en)Pd(NO_3)$_2$] (17.7 μmol) was stirred with **4** (1.5 μmol) and **5** (1.5 μmol) in D_2O/CD_3CN (1:1, 0.6 mL) for 6 h at 70 °C. e) Only **2·5** assembled after **1** (5.9 μmol) was treated with [(en)Pd(NO_3)$_2$] (17.7 μmol) in the presence of **5** (1.5 μmol) and **6** (1.5 μmol). The open circles, filled circles, and squares indicate the signals of **2·4**, **2·5**, and **2·6**, respectively.

Competitive experiments were examined for the guest binding. When **1**, [(en)Pd(NO_3)$_2$], and both **4** and **5** were combined in a ratio of 4:12:1:1 in D_2O/CD_3CN, NMR spectroscopy showed the assembly of **2·4** and **2·5** in a roughly 3:1 ratio after 6 h at 70 °C (Figure 5d). This result indicates that guest **4** is more effectively bound than **5**. In the presence of both **5** and **6**, surprisingly, only the formation of **2·5** was observed (Figure 5e), which indicates that **2·5** is overwhelmingly more stable than **2·6**.

To obtain some insight into the dynamics of guest binding, unsymmetrical guests **7** and **8** were synthesized and inclusion

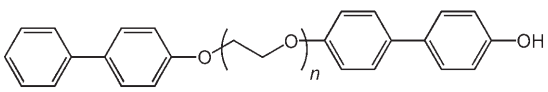

7: $n=5$
8: $n=4$

CHEMISTRY
AN ASIAN JOURNAL

complexes **2·7** and **2·8** were prepared. The desymmetrization of the tubular framework of **2·7** at ambient temperature was observed with NMR spectroscopy (e.g., signals for Hd, Hd′ and Hi, Hi′ in Figure 6b). Upon heating, these pairs of

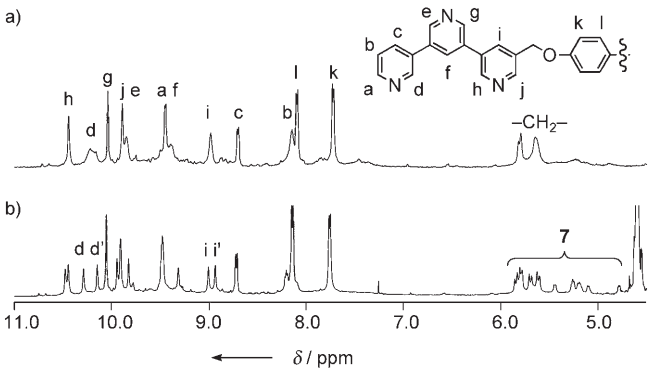

Figure 6. Variable-temperature ^{1}H NMR spectra of **2·7** recorded at a) 54 °C and b) 27 °C (500 MHz, $D_2O/CD_3CN = 1:1$, TMS).

peaks coalesced at 54 °C. The signal coalescence is ascribed to the dynamic guest-binding/dissociation behavior that takes place on the NMR timescale at this coalescence temperature (T_c).[17] From the T_c value, the activation energy was estimated to be 66.6 kJ mol^{-1}. Interestingly, the T_c of **2·8** was much higher (79 °C, Figure 7a), and the evaluated activation energy was 71.1 kJ mol^{-1}. This fact suggests that strand **8** is accommodated within the tube more tightly than **7** despite the small difference in the chain lengths of **7** and **8**.

In each case, the addition of an excess amount of the guest made no change to T_c, which strongly indicates that the guest can be replaced by a second one through an S_N1-like pathway, in contrast to the mechanism for the case of the use of previously reported shorter tubes.[17c]

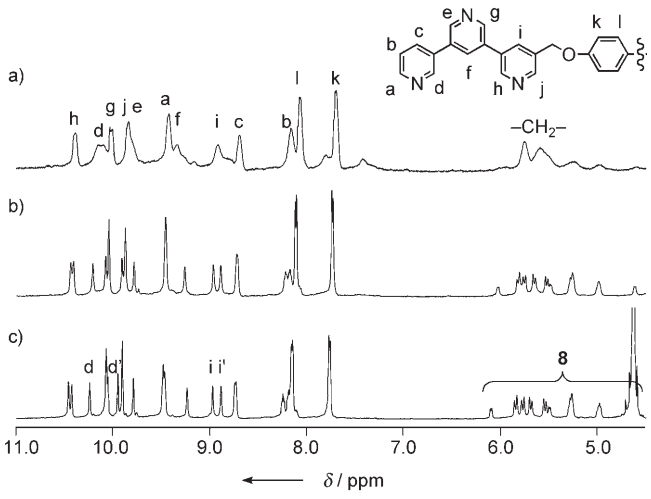

Figure 7. Variable-temperature ^{1}H NMR spectra of **2·8** recorded at a) 79 °C, b) 54 °C, and c) 27 °C (500 MHz, $D_2O/CD_3CN = 1:1$, TMS).

Electrochemical Behavior of a Redox-Active Molecule within the Nanotube

With 24-valent cationic charge, tube **2** is capable of binding neutral and anionic guests strongly, but not cationic guests. We designed redox-active strand **9** with two TTF units linked by an oligo(ethyleneoxide) spacer. As TTF generates stable cation radical $TTF^{+\cdot}$ and dication TTF^{2+} upon oxidation, the cationic charge of guest **9** can be modulated by an electrochemical method.

A unique redox phenomenon of **9** was observed in the channel of **2**.[18] When the cyclic voltammogram of **2·9** was recorded in aqueous $NaNO_3$ solution at a scan rate of 100 mV s^{-1} in the range −200 to 1000 mV, only one anodic peak was observed at the anodic peak potential ($E_{p,a}$) of 764 mV (vs. Ag/AgCl). However, two cathodic peaks were observed at $E_{p,c} = 564$ and 224 mV, which are typical values for the $TTF^{2+}/TTF^{+\cdot}$ and $TTF^{+\cdot}/TTF$ reductions (Figure 8).[19] The unusually high overpotential for the oxi-

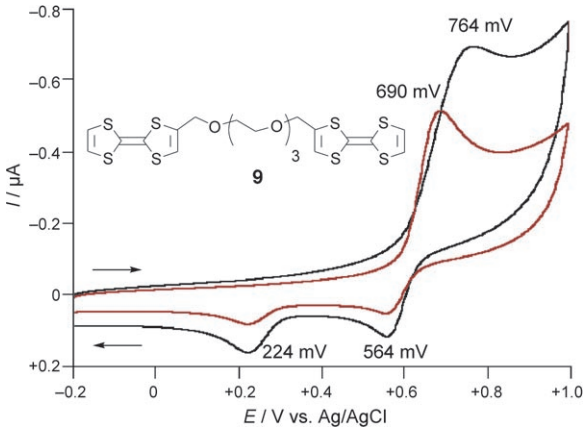

Figure 8. Cyclic voltammogram of **2·9** at scan rates of 100 mV s^{-1}(black) and 50 mV s^{-1}(red) (glassy carbon disk electrode vs. Ag/AgCl, 30 mM $NaNO_3$ in H_2O, room temperature).

dation of guest **9** can be explained by assuming the kinetic stabilization of the internal TTF species (TTF(in)) by the tube. In the tube, the TTF(in) guest is kinetically protected, and the in–out equilibration can be ignored until the potential is swept to around 600 mV at 100 mV s^{-1}. Above this potential, however, the in–out equilibration can no longer be ignored, and the expelled guest is immediately and subsequently oxidized in a two-electron process with $E_{p,a}$ = 764 mV into the TTF^{2+}(out) species. The species obtained after one-electron oxidation, $TTF^{+\cdot}$, is not observed because the potential is already higher than that of TTF^{2+}(out)/$TTF^{+\cdot}$(out) (Scheme 3).[20] At a scan rate of 50 mV s^{-1}, the guest was oxidized in a two-electron process with a lower $E_{p,a}$ value of 690 mV, because the guest is kinetically protected only up to the lower potential at the lower scan rate. The reduction processes should take place outside the tube. Thus, the $E_{p,c}$ values do not depend on the sweep rate because there is no kinetic stabilization by the tube outside it.

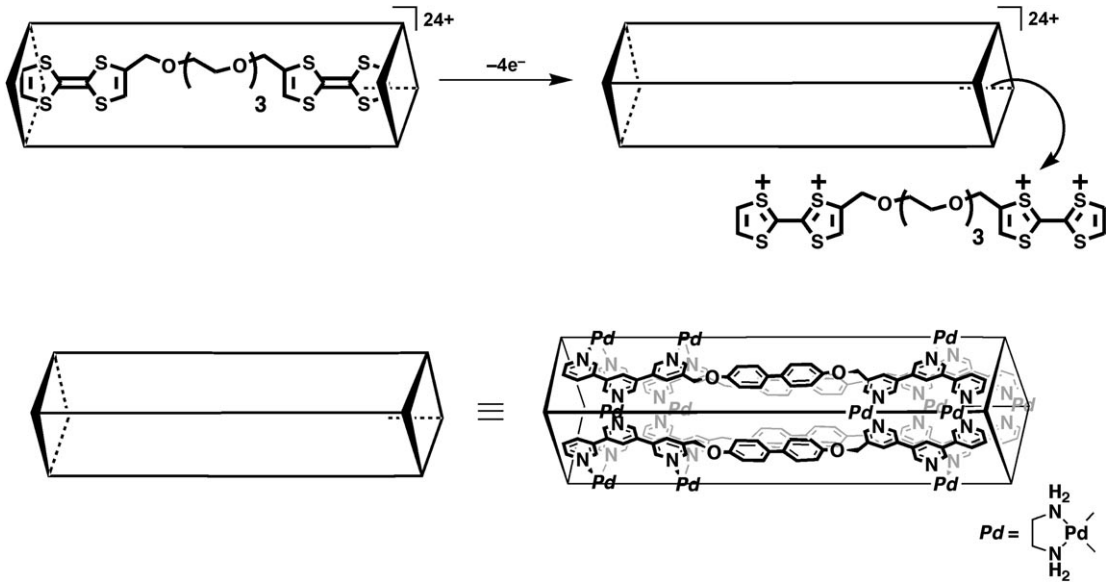

Scheme 3. Dynamic behavior of complex **2·9**.

Hence, the reductions took place stepwise at ordinary $E_{p,c}$ values of 564 (TTF^{2+}(out)/$TTF^{+\cdot}$(out)) and 224 mV ($TTF^{+\cdot}$(out)/TTF(out)).

Conclusions

We have shown the discrete self-assembly of the hitherto longest, crystallographically defined tube structure with a length of 3.5 nm. Size-selective inclusion of molecules and unique behavior of guests within the tube are attractive applications. We emphasize that this nanoscopic self-assembly and potential functions of the coordination nanotube are achieved by the precise design of not only the components and the tube structure but also the efficient assembly pathway by means of a template.

Experimental Section

General

All chemicals were of reagent grade and used without further purification. NMR spectral data were recorded either on Bruker DRX 500 or JEOL AL-300 spectrometers. These data were collected at ambient temperature unless otherwise noted, and the chemical shift values reported here are with respect to external TMS standard. CSI-MS data were measured on a four-sector (BE/BE) tandem mass spectrometer (JMS-700C, JEOL). Electrochemical experiments were performed in aqueous solutions of $NaNO_3$ (30 mM) with a BAS100B/W electrochemical analyzer (Bioanalytical Systems). A glassy carbon working electrode, a Pt counter-electrode, and an Ag/AgCl reference electrode were utilized in a single-component cell.

X-ray crystallographic measurement was performed on a PF-AR NW2 beamline at the High-Energy Accelerator Research Organization (KEK), Japan. Crystal data for **2·3**: orthorhombic, space group *Fdd*2, λ(synchrotron) = 0.68900 Å, T = 88(2) K, a = 49.2540(12), b = 122.86(4), c = 27.6620(5) Å, V = 167395(55) Å^3, Z = 16, d_{calcd} = 1.138 Mg m^{-3}. CCDC-238715 contains the supplementary crystallographic data for this paper. These data can be obtained free of charge from the Cambridge Crystallographic Data Centre at www.ccdc.cam.uk/data_request.cif.

Syntheses

1: The alkylation of 4,4′-dihydroxybiphenyl (0.63 g, 3.4 mmol) with 3-bromo-5-chloromethylpyridine hydrochloride (2.5 g, 10.2 mmol) was carried by treatment with K_2CO_3 (2.8 g, 20.0 mmol) in dry DMF (25 mL) for 5 days at 70 °C. After addition of water, the reaction mixture was extracted with $CHCl_3$. The combined extract was dried over Na_2SO_4 and evaporated, and the residue was purified by column chromatography (silica gel, $CHCl_3$) to give 4,4′-bis[(5-bromo-3-pyridyl)methoxy]biphenyl (**10**) in 62% yield. Subsequently, a mixture of **10** (1.5 g, 2.85 mmol), 3-tributylstannyl-5,3′-bipyridine (3.8 g, 8.55 mmol), and $[Pd(PPh_3)_4]$ (1.0 g, 0.87 mmol) in dry toluene (90 mL) was heated under reflux for 5 days. The mixture was filtered and the precipitate was purified by column chromatography (silica gel, $CHCl_3$/MeOH = 15:1) to give **1** as a white powder (0.73 g, 38% yield). M.p.: 299–304 °C; IR (KBr): $\tilde{\nu}$ = 3036, 2898, 1613, 1573, 1501, 1371, 1276, 1252, 1019, 875 cm^{-1}; ^{1}H NMR (500 MHz, $CDCl_3$/CD_3OD = 3:1): δ = 8.93–8.86 (m, 8H), 8.77 (s, 2H), 8.66 (d, J = 3.5 Hz, 2H), 8.26 (s, 2H), 8.22 (s, 2H), 8.13 (d, J = 8.5 Hz, 2H), 7.58 (dd, J = 8.5, 3.5 Hz, 2H), 7.54 (d, J = 9.0 Hz, 4H), 7.10 (d, J = 9.0 Hz, 4H), 5.30 ppm (s, 4H); ^{13}C NMR (125 MHz, CD_3COOD): δ = 158.1, 147.1, 146.7, 146.6, 145.7, 145.6, 139.0, 137.0, 135.9, 134.6, 134.4, 134.3, 134.2, 134.0, 128.2, 126.0, 115.8, 67.3 ppm; HRMS (EI): m/z calcd for $C_{44}H_{33}N_6O_2$: 677.2665 $[M+H]^+$; found: 677.2704.

3: $SOCl_2$ (0.087 mL, 1.19 mmol) was added dropwise to a mixture of 2-anthracenecarboxylic acid (0.25 g, 1.12 mmol) and dry pyridine (0.18 mL, 2.24 mmol) in dry THF (10 mL) cooled to 0 °C with an ice bath. The reaction was allowed to warm to room temperature and stirred for 12 h. Then, diethylene glycol (0.054 g, 0.51 mmol) in dry THF (10 mL) was added, and the mixture was stirred at room temperature for 2 days. After addition of water (100 mL), the reaction mixture was extracted with $CHCl_3$. The organic phase was dried over Na_2SO_4 and evaporated. The crude product was purified by column chromatography (silica gel, $CHCl_3$) to give **3** as a yellow powder (60.0 mg, 23% yield). M.p.: 179–182 °C; IR (KBr): $\tilde{\nu}$ = 2922, 2854, 1711, 1313, 1280, 1235, 1087, 924, 880 cm^{-1}; ^{1}H NMR (500 MHz, $CDCl_3$): δ = 8.72 (s, 2H), 8.32 (s, 2H), 8.21 (S, 2H), 7.93 (d, J = 8.8 Hz, 2H), 7.91 (d, J = 7.0 Hz, 2H), 7.83 (d, J = 8.2 Hz, 2H), 7.81 (d, J = 8.8 Hz, 2H), 7.48 (dd, J = 8.2, 7.0 Hz, 2H), 7.42 (dd, J = 8.2, 7.0 Hz, 2H), 4.63 (t, J = 4.5 Hz, 4H), 4.00 ppm (t, J = 4.5 Hz, 4H); ^{13}C NMR (125 MHz, $CDCl_3$): δ = 166.7, 133.0, 132.5, 132.4, 131.9, 130.2, 128.6, 128.4, 128.3, 128.1, 126.7, 126.5, 126.1, 125.7, 123.9, 69.3,

64.0 ppm; elemental analysis: calcd (%) for $C_{34}H_{26}O_5 \cdot H_2O$: C 76.68, H 5.30; found: C, 76.74, H, 5.01.

Self-assembly of **2·3**: Ligand **1** (4.0 mg, 5.9 μmol) and [(en)Pd(NO_3)$_2$] (5.2 mg, 17.7 μmol) were combined in H_2O/CH_3CN (1:1, 0.6 mL) and stirred for 2 h at 70 °C. Powdered **3** (0.8 mg, 1.5 μmol) was added to this solution, and the mixture was stirred for 6 h at 70 °C. After filtration, the solution was evaporated. Complex **2·3** was obtained quantitatively as a white powder. M.p.: 275 °C (decomp.); ^{1}H NMR (500 MHz, D_2O/CD_3CN = 1:1): δ = 10.28 (s, 4H), 9.98 (s, 4H), 9.88 (s, 4H), 9.81 (s, 4H), 9.72 (s, 4H), 9.49 (d, J = 5.6 Hz, 4H), 8.97 (s, 4H), 8.73 (d, J = 7.4 Hz, 4H), 8.52 (s, 4H), 8.27 (dd, 7.4, 5.6 Hz, 4H), 8.19 (d, J = 7.6 Hz, 8H), 7.76 (d, J = 8.1 Hz, 1H), 7.70 (d, J = 7.6 Hz, 8H), 7.39 (s, 1H), 6.96 (d, J = 7.5 Hz, 1H), 6.53 (s, 1H), 6.33 (s, 1H), 5.62 (d, J = 12.0 Hz, 4H), 5.36 (dd, J = 8.1, 8.1 Hz, 1H), 5.27–5.25 (m, 5H), 5.03 (d, J = 8.1 Hz, 1H), 4.98 (d, J = 8.1 Hz, 1H), 3.23–3.21 (m, 50H), 2.23 ppm (t, J = 8.1 Hz, 2H); ^{13}C NMR (125 MHz, D_2O/CD_3CN = 1:1): δ = 176.7, 158.1, 153.3, 151.2, 150.9, 150.6, 149.5, 149.4, 145.5, 139.5, 138.1, 135.7, 135.5, 134.4, 134.2, 133.6, 132.9, 131.4, 130.5, 129.4, 128.1, 127.8, 127.5, 126.3, 125.1, 123.9, 116.0, 66.6, 62.8, 48.1, 47.3, 46.1 ppm (some signals were not clearly observed owing to low signal-to-noise ratio); MS (CSI) of **2·3**·(NO_3)$_{24}$: m/z = 1614.5 $[M-(NO_3^-)_4]^{4+}$, 1278.9 $[M-(NO_3^-)_5]^{5+}$, 1055.3 $[M-(NO_3^-)_6]^{6+}$, 895.7 $[M-(NO_3^-)_7]^{7+}$.

4: A mixture of 4-phenylphenol (0.21 g, 1.25 mmol), 1,8-ditosyloxy-3,6-dioxaoctane (0.23 g, 0.50 mmol), and K_2CO_3 (0.35 g, 2.5 mmol) in dry DMF (4 mL) was stirred at 100 °C for 1 day. After addition of water, the reaction mixture was extracted with $CHCl_3$. The combined extract was dried over anhydrous Na_2SO_4 and evaporated under reduced pressure, and the residue was purified by column chromatography (silica gel, $CHCl_3$) to give **4** as a white powder (80 mg, 35% yield). M.p.: 126–128 °C; IR (KBr): $\tilde{\nu}$ = 2919, 2886, 1606, 1524, 1489, 1286, 1257, 1202, 1144, 1063, 988, 926, 837, 758, 688 cm^{-1}; ^{1}H NMR (500 MHz, $CDCl_3$): δ = 7.53 (d, J = 7.5 Hz, 4H), 7.50 (d, J = 8.6 Hz, 4H), 7.40 (dd, J = 7.7, 7.6 Hz, 4H), 7.29 (t, J = 7.4 Hz, 2H), 6.98 (d, J = 8.6 Hz, 4H), 4.17 (dd, J = 4.9, 4.8 Hz, 4H), 3.89 (dd, J = 5.0, 4.6 Hz, 4H), 3.89 ppm (s, 4H); ^{13}C NMR (75 MHz, $CDCl_3$): δ = 158.4, 140.8, 133.9, 128.7, 128.1, 126.7, 126.7, 114.9, 70.9, 69.8, 67.5 ppm; elemental analysis: calcd (%) for $C_{30}H_{30}O_4$: C 79.27, H 6.65; found: C, 79.00, H, 6.79.

5: Strand molecule **5** was prepared similarly to **4** by using 1,1-ditosyloxy-3,6,9-trioxaundecane. Column chromatography (silica gel, $CHCl_3$ and hexane/EtOAc = 3:1) and gel permeation chromatography ($CHCl_3$) gave **5** in 69% yield. M.p.: 116–118 °C; IR (KBr): $\tilde{\nu}$ = 2874, 1604, 1522, 1491, 1453, 1289, 1250, 1196, 1107, 1061, 960, 842, 766, 698 cm^{-1}; ^{1}H NMR (500 MHz, $CDCl_3$): δ = 7.53 (d, J = 7.5 Hz, 4H), 7.50 (d, J = 8.6 Hz, 4H), 7.40 (dd, J = 7.9, 7.5 Hz, 4H), 7.29 (t, J = 7.3 Hz, 2H), 6.97 (d, J = 8.7 Hz, 4H), 4.16 (dd, J = 5.1, 4.6 Hz, 4H), 3.88 (dd, J = 5.0, 4.8 Hz, 4H), 3.73 ppm (m, 8H); ^{13}C NMR (75 MHz, $CDCl_3$): δ = 158.3, 140.7, 133.9, 128.7, 128.1, 126.7, 126.6, 114.9, 70.8, 70.7, 69.7, 67.5 ppm; elemental analysis: calcd (%) for $C_{32}H_{34}O_5$: C 77.08, H, 6.87; found: C 76.88, H, 6.98.

6: In a similar way, strand molecule **6** was prepared in 57% yield. M.p.: 112–113 °C; IR (KBr): $\tilde{\nu}$ = 2943, 2877, 1604, 1523, 1491, 1250, 1198, 1111, 1065, 954, 924, 837, 766, 699 cm^{-1}; ^{1}H NMR (500 MHz, $CDCl_3$): δ = 7.54 (d, J = 6.9 Hz, 4H), 7.50 (d, J = 8.8 Hz, 4H), 7.40 (dd, J = 8.2, 7.6 Hz, 4H), 7.29 (t, J = 7.6 Hz, 2H), 6.98 (d, J = 8.8 Hz, 4H), 4.16 (dd, J = 5.1, 4.4 Hz, 4H), 3.87 (dd, J = 5.1, 4.4 Hz, 4H), 3.73 (ddd, J = 6.9, 3.2, 1.9 Hz, 4H), 3.70–3.67 ppm (m, 8H); ^{13}C NMR (75 MHz, $CDCl_3$): δ = 158.3, 140.7, 133.9, 128.7, 128.1, 126.7, 126.6, 114.9, 76.6, 70.8, 70.6, 69.7, 67.5 ppm; elemental analysis: calcd (%) for $C_{34}H_{38}O_6 \cdot 0.2H_2O$: C 74.76, H, 7.09; found: C, 74.75, H, 7.05.

2·4: ^{1}H NMR (500 MHz, D_2O/CD_3CN = 1:1): δ = 10.39 (s, 8H), 10.02 (s, 8H), 10.00 (s, 8H), 9.88 (s, 8H), 9.75 (s, 8H), 9.47 (d, J = 5.7 Hz, 8H), 9.15 (s, 8H), 8.84 (s, 8H), 8.73 (d, J = 7.9 Hz, 8H), 8.24 (dd, J = 6.8, 6.7 Hz, 8H), 8.13 (d, J = 8.0 Hz, 16H), 7.73(d, J=7.9 Hz, 16H), 6.55 (d, J = 7.7 Hz, 4H), 5.72 (d, J = 12.9 Hz, 8H), 5.50 (d, J = 7.7 Hz, 4H), 5.40 (d, J = 12.2 Hz, 12H), 5.10 (t, J = 7.1 Hz, 2H), 4.74 (br, 4H), 3.67 (br, 4H), 3.37–3.25 (m, 48H), 2.64 (s, 4H), 2.42 ppm (br, 4H).

2·5: ^{1}H NMR (500 MHz, D_2O/CD_3CN = 1:1): δ = 10.41 (s, 8H), 10.10 (s, 8H), 10.04 (s, 8H), 9.90 (s, 8H), 9.80 (s, 8H), 9.47 (d, J = 5.7 Hz, 8H), 9.29 (s, 8H), 8.89 (s, 8H), 8.71 (d, J = 7.5 Hz, 8H), 8.22 (dd, J = 6.8, 6.7 Hz, 8H), 8.13 (d, J = 7.8 Hz, 16H), 7.74(d, J=7.8 Hz, 16H), 5.82 (d, J = 7.8 Hz, 4H), 5.78 (d, J = 13.0 Hz, 8H), 5.59 (d, J = 13.0 Hz, 8H), 5.45 (d, J = 7.4 Hz, 4H), 5.41 (t, J = 7.1 Hz, 2H), 5.18 (d, J = 6.8 Hz, 4H), 5.07 (dd, J = 7.1, 6.8 Hz, 4H), 3.66 (br, 4H), 3.37–3.25 (m, 48H), 2.93 (br, 4H), 2.73 (br, 4H), 2.55 ppm (br, 4H).

2·6: ^{1}H NMR (500 MHz, D_2O/CD_3CN = 1:1): δ = 10.41 (s, 8H), 10.12 (s, 8H), 10.01 (s, 8H), 9.88 (s, 8H), 9.79 (s, 8H), 9.44 (d, J = 5.2 Hz, 8H), 9.30 (s, 8H), 8.91 (s, 8H), 8.68 (d, J = 7.1 Hz, 8H), 8.14 (dd, J = 7.1, 5.2 Hz, 8H), 8.08 (d, J = 5.6 Hz, 16H), 7.71(d, J=5.6 Hz, 16H), 5.76 (d, J = 12.5 Hz, 12H), 5.69 (br, 2H), 5.58 (d, J = 12.5 Hz, 8H), 5.41 (br, 4H), 5.25 (br, 8H), 3.45 (br, 4H), 3.35–3.07 (m, 58H), 2.94 ppm (br, 4H).

7: The alkylation of 4-phenylphenol with 1,14-ditosyloxy-3,6,9,12-tetroxatetradecane gave precursor **11** (44%), which was subsequently added to a mixture of 4,4′-dihydroxy-1,1′-biphenyl (73 mg, 0.4 mmol) and K_2CO_3 (0.11 g, 0.8 mmol) in dry DMF (3 mL). The reaction mixture was stirred

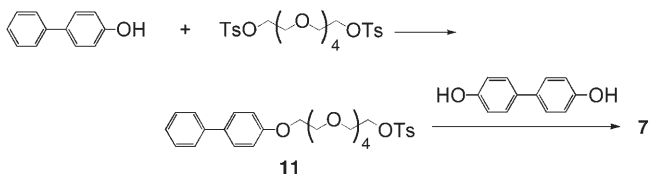

11

at 100 °C for 1.5 days. After addition of hydrochloric acid (0.1 mol L^{-1}), the mixture was extracted with $CHCl_3$. The combined extract was dried over anhydrous Na_2SO_4 and evaporated under reduced pressure, and the residue was purified by column chromatography (silica gel, CHCl3) to give 7 in 45% yield. M.p.: 65–69 °C; IR (KBr): $\tilde{\nu}$ = 3348, 2875, 1608, 1501, 1453, 1271, 1248, 1129, 1065, 950, 824, 764, 695 cm^{-1}; ^{1}H NMR (500 MHz, CDCl3): δ = 7.53 (d, J = 7.4 Hz, 2H), 7.49 (d, J = 8.7 Hz, 2H), 7.40 (dd, J = 7.8, 7.6 Hz, 2H), 7.38 (d, J = 8.9 Hz, 2H), 7.36 (d, J = 8.6 Hz, 2H), 7.29 (t, J = 7.3 Hz, 1H), 6.96 (d, J = 8.7 Hz, 2H), 6.89 (d, J = 8.7 Hz, 2H), 6.87 (d, J = 8.5 Hz, 2H), 5.46 (s, 1H), 4.14 (dd, J = 5.0, 4.7 Hz, 2H), 4.09 (dd, J = 5.0, 4.7 Hz, 2H), 3.85 (dd, J = 5.0, 4.8 Hz, 2H), 3.85 (dd, J = 5.0, 4.8 Hz, 2H), 3.73 (dd, J = 3.0, 2.5 Hz, 2H), 3.72 (dd, J = 2.6, 2.5 Hz, 2H), 3.69 ppm (m, 8H); ^{13}C NMR (75 MHz, $CDCl_3$): δ = 158.3, 157.8, 155.0, 140.8, 133.9, 133.5, 133.2, 128.7, 128.1, 127.8, 127.6, 126.7, 126.7, 115.7, 114.9, 114.8, 70.8, 70.8, 70.7, 70.6, 69.8, 69.7, 67.5, 67.4 ppm; elemental analysis: calcd (%) for $C_{34}H_{38}O_7 \cdot 0.3H_2O$: C 72.40, H 6.90; found: C 72.37, H 6.99.

8: In a similar way, guest **8** was prepared in 34% yield. M.p.: 119–121 °C; IR (KBr): $\tilde{\nu}$ = 3386, 2923, 2879, 1609, 1501, 1455, 1249, 1119, 1099, 1069, 954, 822, 764, 695 cm^{-1}; ^{1}H NMR (500 MHz, $CDCl_3$): δ = 7.53 (d, J = 7.7 Hz, 2H), 7.50 (d, J = 8.6 Hz, 2H), 7.41 (m, 6H), 7.29 (t, J = 7.3 Hz, 1H), 6.97 (d, J = 8.5 Hz, 2H), 6.94 (d, J = 8.6 Hz, 2H), 6.86 (d, J = 8.4 Hz, 2H), 4.86 (s, 1H), 4.16 (dd, J = 5.6, 4.7 Hz, 2H), 4.15 (dd, J = 5.5, 4.7 Hz, 2H), 3.89 (br, 4H), 3.73 ppm (m, 8H); ^{13}C NMR (75 MHz, $CDCl_3$): δ = 158.3, 157.8, 154.8, 140.7, 133.9, 133.5, 133.4, 128.7, 128.1, 127.8, 127.6, 126.7, 126.6, 115.6, 114.9, 114.8, 70.8, 70.7, 70.7, 69.8, 69.8, 67.5, 67.4 ppm; elemental analysis: calcd (%) for $C_{32}H_{34}O_6$: C 74.69, H 6.86; found: C 74.43, H 6.79.

2·7: ^{1}H NMR (500 MHz, D_2O/CD_3CN = 1:1) δ = 10.48 (s, 4H), 10.45 (s, 4H), 10.29 (s, 4H), 10.15 (s, 4H), 10.06 (s, 8H), 9.95 (s, 4H), 9.91 (s, 8H), 9.83 (s, 4H), 9.48 (br, 12H), 9.32 (s, 4H), 9.01 (s, 4H), 8.94 (s, 4H), 8.72 (d, J = 7.8 Hz, 8H), 8.21 (dd, J = 6.7, 6.4 Hz, 4H), 8.14 (d, J = 7.6 Hz, 16H), 8.13 (br, 4H), 7.76 (d, J = 7.2 Hz, 16H), 5.85 (d, J = 12.6 Hz, 4H), 5.79 (d, J = 11.7 Hz, 4H), 5.70 (d, J = 12.5 Hz, 4H), 5.62 (d, J = 12.2 Hz, 4H), 5.45 (d, J = 5.9 Hz, 2H), 5.26 (br, 3H), 5.20 (br 4H), 5.11 (d, J = 7.6 Hz, 2H), 4.78 (d, J = 5.7 Hz, 2H), 4.56 (br, 2H), 3.56 (br 2H), 3.41–3.27 (m, 52H), 3.06 (br, 2H), 3.02 (br, 4H), 2.96 (br, 4H), 2.89 ppm (br, 4H).

2·8: ^{1}H NMR (500 MHz, D_2O/CD_3CN = 1:1): δ = 10.46 (s, 4H), 10.43 (s, 4H), 10.24 (s, 4H), 10.07 (s, 8H), 10.05 (s, 4H), 9.95 (s, 4H), 9.91 (s, 8H), 9.79 (s, 4H), 9.48 (s, 4H), 9.47 (d, J = 6.9 Hz, 8H), 9.24 (s, 4H), 8.97 (s, 4H), 8.89 (s, 4H), 8.74 (d, J = 6.2 Hz, 8H), 8.25 (dd, J = 6.4, 6.3 Hz, 4H),

8.19 (dd, J=6.4, 6.3 Hz, 4H), 8.15 (d, J=7.2 Hz, 16H), 7.76 (d, J= 7.1 Hz, 16H), 6.10 (d, J=7.1 Hz, 2H), 5.85 (d, J=12.6 Hz, 4H), 5.77 (d, J=12.9 Hz, 4H), 5.69 (d, J=12.8 Hz, 4H), 5.54 (d, J=12.7 Hz, 4H), 5.49 (d, J=7.4 Hz, 2H), 5.27 (br, 7H), 4.98 (br, 4H), 4.59 (br, 2H), 3.72 (br, 2H), 3.46 (br, 2H), 3.41–3.27 (m, 50H), 2.83 (br, 2H), 2.70 (br, 2H), 2.60 (br, 2H), 2.57 (br, 2H), 2.43 ppm (br, 2H).

9: NaH (60% in oil, 30 mg, ≈0.73 mmol) was added to solution of 4-(hydroxymethyl)tetrathiafulvalene[21] (85.0 mg, 0.36 mmol) in dry THF (5 mL), and the mixture was stirred for 1 h at room temperature under argon. 1,8-Ditosyloxy-3,6-dioxaoctane (66.0 mg, 0.14 mmol) in dry THF (2 mL) was added, and the mixture was stirred under reflux for 12 h. After cooling, H_2O was slowly added. THF was removed under reduced pressure, and the mixture was extracted with $CHCl_3$. The combined extract was dried over anhydrous Na_2SO_4 and evaporated, and the residue was purified by column chromatography (silica gel, $CHCl_3$) to give **9** as a yellow viscous oil in 78% yield. IR (KBr): $\tilde{\nu}$=3063, 2864, 1675, 1524, 1457, 1348, 1289, 1250, 1114, 1081, 1033, 846, 795, 777, 648 cm^{-1}; ^1H NMR (500 MHz, $CDCl_3$): δ=6.30 (s, 4H), 6.23 (s, 2H), 4.29 (s, 4H), 3.65 ppm (m, 12H); ^{13}C NMR (125 MHz, $CDCl_3$): δ=134.6, 119.1, 119.0, 116.3, 110.8, 110.0, 70.7, 70.6, 69.3, 68.2 ppm; elemental analysis: calcd (%) for $C_{20}H_{22}O_4S_8$: C 41.21, H 3.80; found: C 41.49, H, 3.94.

2·9: This was prepared from tube **2·5** by a facile guest-exchange process. A small excess of **9** was added to a solution of **2·5** (1.5 μmol) in H_2O/CH_3CN (1:1, 1.0 mL), and the mixture was stirred at room temperature for 15 min. After filtration, the solution was evaporated to give **2·9** in 97% yield. ^1H NMR (500 MHz, D_2O/CD_3CN=1:1): δ=10.34 (s, 8H), 9.99 (s, 8H), 9.92 (s, 8H), 9.83 (s, 8H), 9.67 (s, 8H), 9.32 (d, J=5.0 Hz, 16H), 8.94 (s, 8H), 8.61 (d, J=5.0 Hz, 8H), 8.04 (t, J=5.0 Hz, 8H), 7.96 (d, J=8.0 Hz, 16H), 7.57(d, J=7.5 Hz, 16H), 5.70 (d, J=13.2 Hz, 8H), 5.51 (d, J=12.0 Hz, 8H), 5.50 (br, 4H), 5.46 (s, 2H), 3.51 (br, 4H), 3.34–3.06 (m, 52H), 2.05 (br, 4H), 1.99 ppm (s, 4H).

Acknowledgements

We thank S. Adachi (KEK) for supporting the X-ray measurements. T.Y. is grateful for a JSPS Research Fellowship for Young Scientists. This work was approved by the Photon Factory Program Advisory Committee (Proposal No. 2003G186).

[1] a) Y. Jiang, A. Lee, J. Chen, M. Cadene, B. T. Chait, R. MacKinnon, *Nature* **2002**, *417*, 515; b) E. Gouaux, R. MacKinnon, *Science* **2005**, *310*, 1461.

[2] S. Iijima, *Nature* **1991**, *354*, 56.

[3] a) A. Harada, J. Li, M. Kamachi, *Nature* **1993**, *364*, 516; b) A. Harada, M. Okada, Y. Kawaguchi, M. Kamachi, *Polym. Adv. Technol.* **1999**, *10*, 3.

[4] a) M. R. Ghadiri, J. R. Granja, R. A. Milligan, D. E. McRee, N. Khazanovich, *Nature* **1993**, *366*, 324; b) J. D. Hartgerink, T. D. Clark, M. R. Ghadiri, *Chem. Eur. J.* **1998**, *4*, 1367; c) W. S. Horne, C. D. Stout, M. R. Ghadiri, *J. Am. Chem. Soc.* **2003**, *125*, 9372.

[5] a) N. Sakai, K. C. Brennan, L. A. Weiss, S. Matile, *J. Am. Chem. Soc.* **1997**, *119*, 8726; b) N. Sakai, S. Matile, *Chem. Commun.* **2003**, 2514; c) N. Sakai, J. Mareda, S. Matile, *Acc. Chem. Res.* **2005**, *38*, 79; d) S. Bhosale, A. L. Sisson, P. Talukdar, A. Fürstenberg, N. Banerji, E. Vauthey, G. Bollot, J. Mareda, C. Röger, F. Würthner, N. Sakai, S. Matile, *Science* **2006**, *313*, 84.

[6] a) T. Shimizu, M. Masuda, H. Minamikawa, *Chem. Rev.* **2005**, *105*, 1401; b) J. H. Jung, Y. Do, Y.-A. Lee, T. Shimizu, *Chem. Eur. J.* **2005**, *11*, 5538; c) N. Kameta, M. Masuda, H. Minamikawa, N. V. Goutev, J. A. Rim, J. H. Jung, T. Shimizu, *Adv. Mater.* **2005**, *17*, 2732.

[7] a) J. P. Hill, W. Jin, A. Kosaka, T. Fukushima, H. Ichihara, T. Shimomura, K. Ito, T. Hashizume, N. Ishii, T. Aida, *Science* **2004**, *304*, 1481; b) W. Jin, T. Fukushima, M. Niki, A. Kosaka , N. Ishii, T. Aida, *Proc. Natl. Acad. Sci. USA* **2005**, *102*, 10801.

[8] a) H. Fenniri, P. Mathivanan, K. L. Vidale, D. M. Sherman, K. Hallenga, K. V. Wood, J. G. Stowell, *J. Am. Chem. Soc.* **2001**, *123*, 3854; b) H. Fenniri, B.-L. Deng, A. E. Ribbe, *J. Am. Chem. Soc.* **2002**, *124*, 11064.

[9] a) M. Aoyagi, K. Biradha, M. Fujita, *J. Am. Chem. Soc.* **1999**, *121*, 7457; b) M. Aoyagi, S. Tashiro, M. Tominaga, K. Biradha, M. Fujita, *Chem. Commun.* **2002**, 2036.

[10] T. Yamaguchi, S. Tashiro, M. Tominaga, M. Kawano, T. Ozeki, M. Fujita, *J. Am. Chem. Soc.* **2004**, *126*, 10818.

[11] M. Tominaga, M. Kato, T. Okano, S. Sakamoto, K. Yamaguchi, M. Fujita, *Chem. Lett.* **2003**, *32*, 1012.

[12] a) R. L. E. Furlan, S. Otto, J. K. M. Sanders, *Proc. Natl. Acad. Sci. USA* **2002**, *99*, 4801; b) J.-M. Kern, J.-P. Sauvage, G. Bidan, B. Divisia-Blohorn, *J. Polym. Sci. Part A: Polym. Chem.* **2003**, *41*, 3470; c) E. N. Guidry, S. J. Cantrill, J. F. Stoddart, R. H. Grubbs, *Org. Lett.* **2005**, *7*, 2129.

[13] a) Y. Tokunaga, D. M. Rudkevich, J. Santamaría, G. Hilmersson, J. Rebek, Jr., *Chem. Eur. J.* **1998**, *4*, 1449; b) V. Berl, M. J. Krische, I. Huc, J.-M. Lehn, M. Schmutz, *Chem. Eur. J.* **2000**, *6*, 1938; c) F. M. Tabellion, S. R. Seidel, A. M. Arif, P. J. Stang, *Angew. Chem.* **2001**, *113*, 1577; *Angew. Chem. Int. Ed.* **2001**, *40*, 1529; d) K. Kumazawa, K. Biradha, T. Kusukawa, T. Okano, M. Fujita, *Angew. Chem.* **2003**, *115*, 4039; *Angew. Chem. Int. Ed.* **2003**, *42*, 3909.

[14] Force-field calculations were carried out with the use of the Cerius^2 Version 3.5 software package, Molecular Simulation Inc., San Diego, CA (USA), **1997**.

[15] a) C.-Y. Su, M. D. Smith, H.-C. zur Loye, *Angew. Chem.* **2003**, *115*, 4219; *Angew. Chem. Int. Ed.* **2003**, *42*, 4085; b) V. G. Organo, A. V. Leontiev, V. Sgarlata. H. V. R. Dias, D. M. Rudkevich, *Angew. Chem.* **2005**, *117*, 3103; *Angew. Chem. Int. Ed.* **2005**, *44*, 3043; c) S. J. Dalgarno, G. W. V. Cave, J. L. Atwood, *Angew. Chem.* **2006**, *118*, 584; *Angew. Chem. Int. Ed.* **2006**, *45*, 570.

[16] B. J. Shorthill, C. T. Avetta, T. E. Glass, *J. Am. Chem. Soc.* **2004**, *126*, 12732.

[17] a) H. Saito, H. Yonemura, H. Nakamura, T. Matsuo, *Chem. Lett.* **1990**, *19*, 535; b) B.-S. Kim, J.-I. Hong, *Chem. Lett.* **2002**, *31*, 336; c) M. Tominaga, S. Tashiro, M. Aoyagi, M. Fujita, *Chem. Commun.* **2002**, 2038.

[18] a) P. M. Schmidt, R. S. Brown, J. H. T. Luong, *Chem. Eng. Sci.* **1995**, *50*, 1867; b) C. M. Cardona, S. Mendoza, A. E. Kaifer, *Chem. Soc. Rev.* **2000**, *29*, 37; c) W.-Y. Sun, T. Kusukawa, M. Fujita, *J. Am. Chem. Soc.* **2002**, *124*, 11570.

[19] All redox potentials were measured with an Ag/AgCl reference electrode.

[20] a) M. Asakawa, P. R. Ashton, V. Balzani, A. Credi, C. Hamers, G. Mattersteig, M. Montalti, A. N. Shipway, N. Spencer, J. F. Stoddart, M. S. Tolley, M. Venturi, A. J. P. White, D. J. Williams, *Angew. Chem.* **1998**, *110*, 357; *Angew. Chem. Int. Ed.* **1998**, *37*, 333; b) V. Balzani, A. Credi, G. Mattersteig, O. A. Matthews, F. M. Raymo, J. F. Stoddart, M. Venturi, A. J. P. White, D. J. Whilliams, *J. Org. Chem.* **2000**, *65*, 1924.

[21] J. Garín, J. Orduna, S. Uriel, A. J. Moore, M. R. Bryce, S. Wegener, D. S. Yufit, J. A. K. Howard, *Synthesis* **1994**, 489.

Received: December 27, 2006

